High-resolution x-ray diffraction study of MnO nanostructured within a MCM-48 silica matrix with a gyroidal system of channels

I. V. Golosovsky,[1] I. Mirebeau,[2] F. Fauth,[3] M. Mazaj,[4] D. A. Kurdyukov,[5] and Yu. A. Kumzerov[5]
[1]*St. Petersburg Nuclear Physics Institute, 188300, Gatchina, St. Petersburg, Russia*
[2]*Laboratoire Léon Brillouin, CE-Saclay, F-91191, Gif-sur-Yvette, France*
[3]*ESRF, Polygone Scientifique Louis Néel, 6 rue Jules Horowitz, 38000, Grenoble, France*
[4]*National Institute of Chemistry, Hajdrihova 19, 1000, Ljubljana, Slovenia*
[5]*A. F. Ioffe Physico-Technical Institute, 194021, St. Petersburg, Russia*
(Received 27 July 2006; revised manuscript received 21 September 2006; published 30 October 2006)

Antiferromagnetic MnO was synthesized within a mesoporous matrix MCM-48 with a gyroidal system of channels. Synchrotron radiation studies reveal that the embedded nanoparticles have a ribbonlike shape and a length of about 53(3) Å. The peculiar diffraction line shape shows the loss of long-range atomic order. In spite of positional disorder, a transition from a cubic structure to a rhombohedral one, similar to the transition known for the bulk, is observed.

DOI: 10.1103/PhysRevB.74.155440 PACS number(s): 61.46.−w, 61.10.Nz

The physics of nanostructured compounds is now a very active field of research. The properties of matter confined to nanometer scale porous media differ from those of the bulk, stimulating studies of such composite materials.

Some years ago we started a systematic investigation of structure and magnetism in the classic antiferromagnet manganese oxide (MnO) confined to different porous media: within a Vycor-type glass matrix with a random network of pores[1] and within MCM-41 type matrices with a regular system of nanochannels.[2–5]

During the past decade a new silicate mesoporous matrix MCM-48 with remarkable properties was synthesized.[6] This matrix is marvelous because the channels piercing its amorphous silica body comply with the symmetry of the cubic space groups.[7,8] The channel wall surface exactly follows the so-called periodic minimal surface, forming a double gyroidal mesostructure with a three-dimensional network of channels running along [100] and [111] directions (see Ref. 9). The system of channels forms two enantiomeric, bicontinuous, branched, self-intersecting volumes separated by an infinite wall [Fig. 1(a)].

Gyroidal structures are known in binary water-lipid systems, diblock copolymers, biological objects and others, where surfactant mesophases with a minimal surface appear under special conditions. The specific shape of the mesophase surface results from the balance between the interfacial energy, which favors a surface with constant minimal curvature and the stretching energy, which favors a planar surface. The simple example of such a mesophase is a thin surfactant layer in the self-arranged mixture of oil and water.[10]

Among the known mesostructured matrices, MCM-48 channel structure is perhaps the most complex one and attracts much attention.[11] The large pore volume, high specific surface area and chemical inertness, together with the ordered high-symmetrical system of channels make this matrix quite promising for many applications. Nothing is known about the physical properties of materials confined within such a matrix.

In the present paper we report the study of the structure of MnO synthesized within the matrix MCM-48, using synchrotron radiation diffraction. The results are compared with results about MnO synthesized within the matrix MCM-41 with a system of parallel channels. Both matrices have the same channel diameter but different topologies.

Experimental details. The host matrix MCM-48 with a gyroidal system of channels was prepared by hydrothermal synthesis in the presence of structure-directing agents: cetyltrimethylammonium bromide, Triton® X-114, and sodium silicate as a silica source in a autoclave at 100 °C for 24 h.[12] The channel diameter was measured by the N_2 adsorption/desorption method at 77 K using Tristar 3000 Micromeritics facility and was found to be 33(3) Å.

To compare the properties of confined nanoparticles in different topologies, the matrix MCM-41 with a channel diameter of 35 Å was prepared by the standard technology.[13] Manganese oxide was crystallized within the channels of both matrices by the "bath deposition method."

High-resolution x-ray diffraction experiments were per-

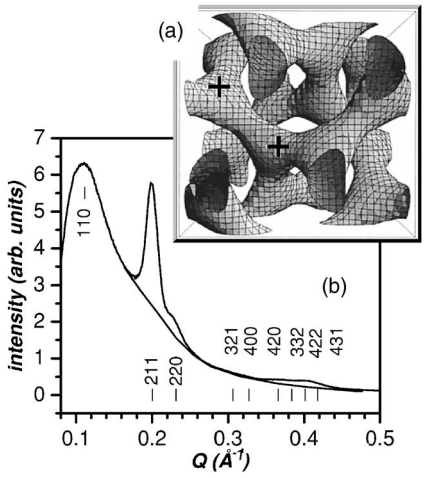

FIG. 1. (a) 3D-bicontinuous, branched, self-intersecting gyroidal system of channels (from Ref. 7); (b) low-angle x-ray diffraction pattern from the MCM-48 matrix. Bars mark the reflection positions.

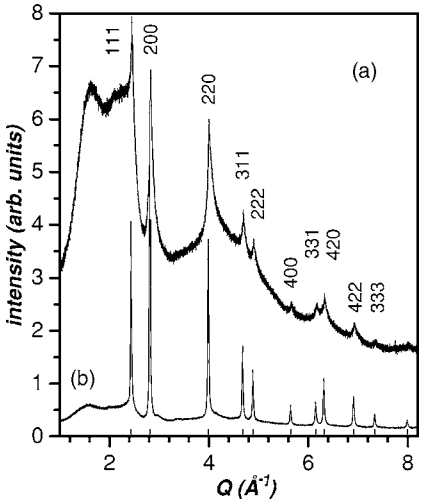

FIG. 2. X-ray diffraction patterns of MnO confined within the matrices MCM-41 (a) and MCM-48 (b) (here the intensity was multiplied by a factor 6) measured at room temperature. Bars mark the reflection positions.

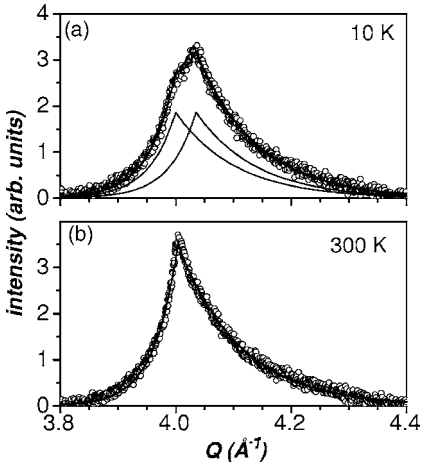

FIG. 3. Fragments of x-ray diffraction patterns around 220 reflection from MnO within the matrix MCM-48 at 10 K (a) and 130 K (b). Two profiles in thin lines correspond to deconvolution of the resulting profile. Thick solid line through the experimental points is a fit with an exponential law (see text).

formed at the beam-station ID31 of the European Synchrotron Radiation Facility with a wavelength of 0.500 Å. To avoid preferred orientation effects, the powder samples sealed in 1 mm diameter quartz capillaries were rotated continuously during the experiment. An Oxford Instruments continuous flow cryostat was used.

Results and discussion. In Fig. 1(b) the diffraction pattern measured at low angles is shown. It is consistent with the diffraction patterns presented in recent reports.[7,8]

The observed reflections can be indexed in the space group $Ia\bar{3}d$, specific to the gyroidal system. In the x-ray diffraction pattern of the carbon replica of the MCM-48 channel system, the 110 reflection, indicative of the space group $I4_132$ without inversion center, was observed.[14] The width of the 110 reflection was similar to the width of the 211 reflection but the 110 reflection was twice stronger.[7,14] In the present case, the 110 reflection seems to be absent, as shown in Fig. 1(b), where we have indicated its expected position. However, we cannot fully ascertain it, due to the reduction of the beam by the beam-stop screen.

The profile analysis yields the value of the unit cell parameter of the channel lattice a_0=79.70(5) Å. From the broadening of the 211 peak the diffraction correlation length was evaluated to 310(5) Å. Note that for the matrix MCM-41 with close channel diameter the corresponding diffraction correlation length deduced from the broadening of the 10 peak from a hexagonal lattice[2] was evaluated to 233(3) Å. It means that the gyroidal system is "more perfect" than the system with parallel channels.

X-ray patterns measured for the matrices MCM-41 and MCM-48 are shown in Fig. 2. The observed Bragg reflections result from MnO crystallized within the channels, while the diffuse background originates from the silica host matrix and some amount of amorphous MnO.[3]

There are some remarkable differences and similarities in these two profiles. First, the large difference in the diffuse background is readily explained by the different ratio of the voids to the total volume of the silica matrix and the different amounts of amorphous MnO. Second, an asymmetric "sawtooth" line shape is observed in both patterns, reflecting the two-dimensional character of the MnO lattice, namely, the ribbonlike shape of the embedded nanoparticles.[2,15] This profile is well known in powder diffraction from layers or different adsorbates on graphite.[16–18]

At the Néel temperature (T_N) of 117 K the bulk MnO undergoes a first order phase transition, accompanied by the onset of long-range antiferromagnetic ordering and a rhombohedral distortion of the cubic lattice.[19] In contrast, a second order transition with the enhanced Néel temperature was observed in all cases of confined MnO.[1,4]

We notice that in one peculiar case, namely, in MnO confined to the matrix MCM-41 with 35 Å channel diameter, the rhombohedral distortion, which appears at the Néel temperature of 120 K, suddenly disappears below about 40 K, showing a new phase transition.[5] In MnO confined within the matrix MCM-48, the temperature evolution of the line shape of the 220 Bragg reflection demonstrates a splitting, which corresponds to the rhombohedral distortions of a cubic lattice exactly as in the bulk, without any new phase transition (Fig. 3). To calculate the temperature dependences of the splitting and the angle of the rhombohedral distortion it is necessary to describe the experimental line shape.

In the matrix MCM-41 with a system of parallel channels the peak asymmetry is different for different reflections, reflecting the strongly anisotropic shape of the embedded nanoparticles [Fig. 2(a)]. In particular, the line shape of the 200 reflection is well described by the pseudo-Voigt function $V=0.81L+0.19G$, where L and G are the Lorentzian and Gaussian contributions, respectively [Fig. 4(a)].

The Rietveld profile analysis of the pattern shows that the contribution to the peak broadening from the inner stresses is negligible. The evaluation of the nanoparticle length (maximal dimension) from the peak broadening gives the value of 260(4) Å.

A very different line shape is observed in the matrix

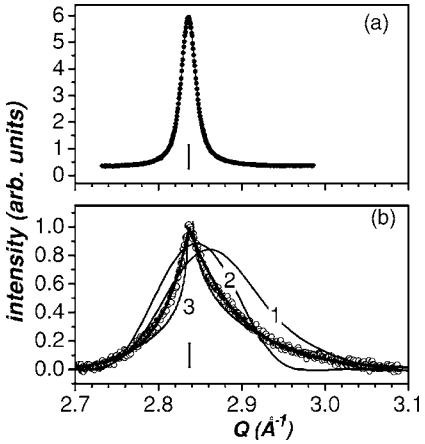

FIG. 4. (a) Profile of the 200 reflection from MnO confined within the matrix MCM-41 measured at 130 K. Thin solid line corresponds to a fit with pseudo-Voigtian. (b) Profiles of the 200 reflection from MnO confined within the matrix MCM-48 measured at 130 K. Open circles: experiment, solid line through the experimental points is a fit with an exponential law; solid lines: (1) a numerical calculation for the ribbon of $50\times30\times5$ Å; (2) a numerical calculation for the ribbon of $50\times30\times20$ Å, (3) a fit with a power law. Overbars mark the reflection position.

MCM-48 with the gyroidal channel system [Fig. 4(b)]. Obviously, a line shape with a sharp maximum cannot be described by the pseudo-Voigt function. Note that the instrumental linewidth in synchrotron radiation experiments is vanishingly small.

By comparing the peak "breadth," defined as the ratio of the integrated intensity to the peak amplitude[20] for the matrices MCM-41 and MCM-48, one can estimate the maximal length of the nanoparticles confined within the matrix MCM-48 to 53(3) Å. This value is close to the evaluation by the Rietveld profile analysis performed for the high-angle pattern (starting from reflection 311), assuming a Lorentzian line shape.

It turns out that the length of 53(3) Å for the nanoparticle confined to the matrix MCM-48 is close to the distance between two nearest branching points [marked in Fig. 1(a) by crosses], which in our case is equal to $a_0/\sqrt{2}=56.3$ Å. It means that the crystallization of MnO nanoparticles completes around these points. So, in the gyroidal system of the channels there is a natural upper limit for the nanoparticle length.

Since the length of a confined nanoribbon is fixed by the branching points, it should be sensitive to the channel diameter due to high symmetry of the gyroidal channel system with a rigid geometry. The observation of a sharp line shape means a very narrow distribution of nanoribbon lengths and suggests that there is no wide distribution of the channel diameters.

The transverse dimension of the embedded nanoribbons cannot be larger than the channel diameter of 33 Å in the matrix MCM-48. We numerically calculated the diffraction profiles by the Debye formula[2] for two nanoribbons with dimensions of $50\times30\times5$ Å and $50\times30\times20$ Å, which limit all reasonable dimensions, since the unit cell parameter for MnO is 4.44 Å. Because the Debye formula includes the powder averaging and the instrumental linewidth is very small, the calculated curves [marked as 1 and 2 in Fig. 4(b)] can be immediately compared with experiment. This comparison shows that the experimental profile cannot be described in the frame of the standard diffraction from a regular lattice.

It can be rigorously shown that in the two-dimensional (2D) lattice, long-range positional order is impossible.[21] On the other hand, there are many examples of partially disordered structures giving rise to Bragg-like peaks in the x-ray diffraction patterns. Shining examples are the diffraction from monolayers of rare gases adsorbed on graphite[16–18] or the diffraction from a smectic liquid crystal,[22] where the diffraction line shape is described in the frame of phonon mechanism, which destroys the atomic periodicity in the low-dimensional lattices.

For such a mechanism the pair correlation function can be described as[23] $\langle \mathbf{U}(\mathbf{R}),\mathbf{U}(0)\rangle \sim R^{-\eta}$. Here $\mathbf{U}(\mathbf{R})$ is the deviation of an atomic position from its average lattice position $\mathbf{R}$. Such a dependence, known as the algebraic decay of correlations, leads to the scattering function $S(\boldsymbol{Q})\sim|\boldsymbol{Q}-\boldsymbol{q}|^{-2+\eta}$, which well describes the peak "tails" in the vicinity of a Bragg reflection with a momentum transfer $\boldsymbol{q}$, while the "divergence" at $\boldsymbol{Q}=\boldsymbol{q}$ is removed by the finite-size effect.[18,24]

The scattering function $S(Q)$, measured in powder diffraction experiment results from the power averaging of all possible orientations of the vector $\boldsymbol{q}$. This averaging depends on the dimensionality of diffracting objects. However in the case of the algebraic decay of correlations, the power law still plausibly fits the tails of the line shape.[18]

Since the phonon mechanism is temperature dependent, the line shape is expected to evolve with temperature. However we did not observe any change of the line shape in the temperature interval 10–300 K. A fit of the experimental profile with a power law (after 2D powder averaging) or by the sum of two profiles resulting from the power law line shape and the Lorentzian line shape, which correspond to partially ordered and fully disordered phases, respectively, as was proposed in Refs. 17 and 18 was not successful. The best fit is shown in Fig. 4(b), curve 3. The peak asymmetry due to the ribbonlike form of nanoparticles was taken into account by different η values at $Q<q$ and $Q>q$.

Surprisingly, an excellent fit of $S(Q)$ around the Bragg position can be achieved with an exponential law, namely, $S(Q)\sim\exp(-|Q-q|\,\eta)$ [the thick line through the experimental points in Figs. 3 and 4(b)]. As before, different values of η at $Q<q$ and $Q>q$ were used, namely, 21.86 and 9.5 Å for the 200 reflection, respectively.

Two important conclusions follow. First, the embedded anisotropic nanoparticles are so small that they cannot be considered as objects with a long-range ordered lattice. Our results suggest that short-range positional order is an intrinsic feature of small confined nanoparticles. Note that the presence of extended structural defects in the nanoparticles of gold with 3 nm size suspended in water was recently confirmed by x-ray diffraction and computer simulation.[25]

Using the exponential law to fit the experimental profiles (Fig. 3) we calculated the angle of the rhombohedral distortion in function of temperature [Fig. 5(a)]. It is seen that the

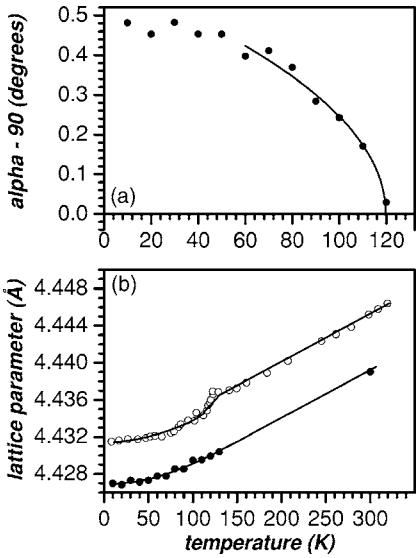

FIG. 5. Temperature dependence of the angle of the rhombohedral distortion (alpha) (a), lattice parameter (b). Open circles corresponds to the bulk MnO. Errors (e.s.d.), if not shown, do not exceed the symbol size. Solid line in (a) is a fit with a power law, in (b) solid lines are the guides for an eye.

distortion in MnO confined within MCM-48 channels shows a usual temperature dependence: it appears at the Néel temperature and gradually increases with decreasing temperature, exactly as in the bulk.

In these calculations we used a unit cell parameter derived from the position of the non-split 200 reflection [Fig. 5(b)]. Similar to the bulk, the lattice parameter decreases with decreasing temperature (Fig. 5). The anomaly at the Néel temperature observed in the bulk is explained by the difference in the next-nearest-neighbors correlation above and below T_N.[26,27] We did not observed such anomaly in the anisotropic MnO nanoparticles confined within the channel type matrices,[2] whereas we observed it in the isotropic MnO nanoparticles confined within a porous glass.[1] It means that spin correlations are very sensitive to the shape of the confined nanoparticle.

The difference in the absolute values of the lattice constants for the bulk and confined MnO is readily explained by the ribbonlike shape of the embedded nanoparticles. It is well known that in the case of a two-dimensional lattice, the maxima of diffraction peaks do not coincide with the nodes in the reciprocal space, which leads to an underestimation of the unit cell parameter.[2,5,15]

A fit of the temperature dependence of the rhombohedral angle with a power law $(1-T/T_N)^{\beta}$ gives $\beta=0.49(6)$ and $T_N=119.7(4)$ K. The last one is close to T_N measured for MnO within the MCM-41 matrix with a system of parallel channels of the same diameter.[4] As well the measured T_N appears to be enhanced with respect to the bulk value.

Assuming that the rhombohedral angle is proportional to the square of the magnetic moment as in the bulk, the exponent in the temperature dependence of the moment turns out to be 0.25(3). This value is characteristic for a low-dimensional magnetic system and coincides with the exponent measured for MnO within the matrix MCM-41 with the same channel diameter.[4] Also, the magnetic transition parameters are the same for MnO within matrices MCM-41 and MCM-48, in spite of their different topologies.

In conclusion, synchrotron radiation diffraction experiments were performed in MnO confined within MCM-48 matrix with a gyroidal system of nanochannels. The crystallized nanoparticles have a ribbonlike shape with a length of about 50 Å and do not show a long-range atomic ordering. It leads to a specific diffraction line shape, which cannot be described in the frame of the known mechanism of the algebraic decay of correlations. In spite of the disordered atomic structure, a phase transition from a cubic structure to a rhombohedral distorted structure is observed, as in the bulk. The parameters of this phase transition are similar to the parameters of the transition observed in MnO within the matrix MCM-41, where the long-range atomic ordering is present.

ACKNOWLEDGMENTS

The authors are grateful to S. L. Ginsburg and S. B. Vakhrushev for a critical reading of the manuscript and fruitful discussions. The work was supported by Grant Nos.: RFBR-04-02-16550, INTAS-2001-0826, and the program RAN "Effect of Atomic-Crystalline and Electronic Structure on the Properties of Condensed Matter."

[1] I. V. Golosovsky, I. Mirebeau, G. André, D. A. Kurdyukov, Yu. A. Kumzerov, and S. B. Vakhrushev, Phys. Rev. Lett. **86**, 5783 (2001).

[2] I. V. Golosovsky, I. Mirebeau, E. Elkaim, D. A. Kurdyukov, and Y. A. Kumzerov, Eur. Phys. J. B **47**, 55 (2005).

[3] I. V. Golosovsky, D. Arčon, Z. Jagličič, P. Cevc, V. P. Sakhnenko, D. A. Kurdyukov, and Y. A. Kumzerov, Phys. Rev. B **72**, 144410 (2005).

[4] I. V. Golosovsky, I. Mirebeau, V. P. Sakhnenko, D. A. Kurdyukov, and Y. A. Kumzerov, Phys. Rev. B **72**, 144409 (2005).

[5] I. V. Golosovsky, I. Mirebeau, F. Fauth, D. A. Kurdyukov, and Y. A. Kumzerov, Phys. Rev. B **74**, 054433,(2006).

[6] C. T. Kresge, M. E. Leonowicz, W. J. Roth, J. C. Vartuli, and J. S. Beck, Nature (London) **359**, 710 (1992).

[7] M. Kaneda, T. Tsubakiyama, A. Carlsson, Y. Sakamoto, T. Ohsuna, O. Terasaki, S. H. Joo, and R. Ryoo, J. Phys. Chem. B **106**, 1256 (2002).

[8] K. Schumacher, P. I. Ravikovitch, A. Du Chesne, A. V. Neimark, and K. K. Unger, Langmuir **16**, 4648 (2000).

[9] M. Wohlgemuth, N. Yufa, J. Hoffman, and E. L. Thomas, Macromolecules **34**, 6083 (2001).

[10] J. Harting, M. J. Harvey, J. Chin, and P. V. Coveney, Comput. Phys. Commun. **165**, 97 (2005).

[11] Bozhi Tian, Xiaoying Liu, L. A. Solovyov, Zheng Liu, Haifeng Yang, Zhendong Zhang, Songhai Xie, Fuqiang Zhang, Bo Tu, Chengzhong Yu, Osamu Terasaki, and Dongyuan Zhao, J. Am. Chem. Soc. **126**, 865 (2004).
[12] W. Zhao and Q. Li, Chem. Mater. **15**, 4160 (2003).
[13] D. Morineau, G. Dossen, and C. Alba-Simionesco, Philos. Mag. B **79**, 1845 (1999).
[14] L. A. Solovyov, V. I. Zaikovskii, A. N. Shmakov, O. V. Belousov, and Ryong Ryoo, J. Phys. Chem. B **106**, 12198 (2002).
[15] B. E. Warren, Phys. Rev. **59**, 693 (1941).
[16] J. K. Kjems, L. Passell, and H. Taub, J. G. Dash, and A. D. Novaco, Phys. Rev. B **13**, 1446 (1976).
[17] P. A. Heiney, P. W. Stephens, R. J. Birgeneau, P. M. Horn, and D. E. Moncton, Phys. Rev. B **28**, 6416 (1983).
[18] P. W. Stephens, P. A. Heiney, R. J. Birgeneau, P. M. Horn, D. E. Moncton, and G. S. Brown, Phys. Rev. B **29**, 3512 (1984).
[19] C. P. Bean and D. S. Rodbell, Phys. Rev. **126**, 104 (1962).
[20] J. I. Langford and D. Loüer, J. Appl. Crystallogr. **15**, 20 (1982).
[21] N. D. Mermin, Phys. Rev. **176**, 250 (1968).
[22] J. Als-Nielsen, J. D. Litster, R. J. Birgeneau, M. Kaplan, C. R. Safinya, A. Lindegaard-Andersen, and S. Mathiesen, Phys. Rev. B **22**, 312 (1980).
[23] Y. Imry and L. Gunther, Phys. Rev. B **3**, 3939 (1971).
[24] P. Dutta and S. K. Sinha, Phys. Rev. Lett. **47**, 50 (1981).
[25] V. Petkov, Yong Peng, G. Williams, Baohua Huang, D. Tomalia, and Yang Ren, Phys. Rev. B **72**, 195402 (2005).
[26] B. Morosin, Phys. Rev. B **1**, 236 (1970).
[27] D. Bloch and R. Maury, Phys. Rev. B **7**, 4883 (1973).